Volume 11, Issue 8, August – 2026 International Journal of Innovative Science and Research Technology
ISSN No:-2456-2165 https://doi.org/10.38124/ijisrt/26aug400

Toward a Digital Twin for Metallurgical Bubbling Fluidized-Bed Roasters A Multiphysics Framework with a Thesis-Derived Start-Up Case

Roger Rumbu[1]; Reggie-John Rumbu[2]

[1]Faculty of Polytechnics, University of Kolwezi, Democratic Republic of the Congo
[2]Wake-Engineering, Sandton, South Africa

Publication Date: 2026/08/20

Abstract: Metallurgical bubbling fluidized-bed roasters couple dense gas–solid hydrodynamics, strongly exothermic sulfide oxidation, interphase heat and mass transfer, solids residence-time distributions, and gas-cleaning constraints. These interactions create a demanding application for digital-twin technology. This perspective proposes a digital-twin framework for such roasters. Zinc-sulfide roasting provides the reference chemistry because it exposes the control conflict among rapid oxidation to ZnO, sulfate formation, thermal uniformity, oxygen availability, zinc-ferrite formation, and agglomeration risk. The framework separates the physical asset, measurement and data-quality layer, high-fidelity multiphysics models, reduced-order online models, state and parameter estimation, diagnostic services, and constrained decision support. A thesis-derived start-up case is integrated as the first operating mode of the twin. In the reported simulations, continuous blowing raised the inert-bed temperature from approximately 298 to 800 K in 1,200 s, while complete-interruption sequences remained within approximately 298–308 K over the first 400 s. These unequal-duration simulations support continuous or near-continuous fluidization as the reference start-up strategy, but they do not establish fuel savings or readiness for concentrate admission. A staged verification and validation programme uses pressure drop, bed expansion, temperature fields, off-gas composition, calcine sulfur speciation, mineralogy, and transient plant tests. The resulting contribution consists of a metallurgically grounded architecture, a cold start-up module supported by preliminary CFD evidence, and testable criteria for progression from numerical comparison to instrumented plant validation.

Keywords: *Bubbling Fluidized Bed; Digital Twin; Zinc-Sulfide Roasting; CFD; Reduced-Order Model; Data Assimilation; Model-Predictive Control; Cold Start-Up; Verification and Validation.*

How to Cite: Roger Rumbu; Reggie-John Rumbu (2026) Toward a Digital Twin for Metallurgical Bubbling Fluidized-Bed Roasters A Multiphysics Framework with a Thesis-Derived Start-Up Case. *International Journal of Innovative Science and Research Technology*, 11(8), 1141-1151. https://doi.org/10.38124/ijisrt/26aug400

I. INTRODUCTION

Bubbling fluidized-bed roasters remain important for oxidizing fine sulfide concentrates because vigorous gas–solid contact supports high reaction rates and relatively uniform bed temperature (Dash et al., 2020; Jarosz and Małecki, 2014). Their apparent thermal uniformity does not remove the underlying complexity. Gas distribution, bubble bypassing, particle segregation, attrition, entrainment, changing mineralogy, oxygen depletion, sulfate stability, and wall heat losses act simultaneously. Small disturbances in feed sulfur, moisture, particle size, or air distribution alter local oxygen potential and heat release. The same disturbance appears in plant signals with different delays. A bed-pressure fluctuation reacts within seconds, an off-gas analyser responds after transport and conditioning delay, and calcine assays arrive much later.

Conventional monitoring displays measured variables but does not infer unmeasured internal states. A digital twin adds a synchronized model of the physical asset, updated with operating data and used for estimation, diagnosis, prediction, or control (Jones et al., 2020; Rasheed et al., 2020). This definition excludes a static CFD model, dashboard, or offline simulator when it lacks managed data exchange and state updating. ISO 23247 provides a manufacturing reference architecture centred on observable manufacturing elements, information exchange, and twin services (ISO, 2021a, 2021b, 2021c). Process-industry implementation also requires conservation laws, thermochemistry, uncertainty treatment, and safeguards against model drift.

The scope covers Eulerian–Eulerian CFD, selected CFD–DEM studies, reduced-order modelling, data assimilation, and constrained control. Experiments, large-

ISSN No:-2456-2165 https://doi.org/10.38124/ijisrt/26aug400

eddy simulation, machine learning, economic assessment, and life-cycle assessment remain outside the evidential claims of the present study. Literature values are distinguished from thesis simulations and proposed validation work. Performance benefits require traceable measurements from an implemented system.

The research questions are: Which metallurgical states determine roaster performance? How should the twin switch among cold start-up, transition to feed admission, autogenous roasting, abnormal operation, and shutdown? Which model hierarchy is accurate enough for design and fast enough for online use? Which measurements render the important states observable? How should physical models and operating data be assimilated? Which tests establish predictive credibility? What safeguards are required before closed-loop optimization?

➤ *Problem Framing*

The objective is to define a scientifically defensible route for establishing a digital twin of a metallurgical bubbling fluidized-bed roaster. The analysis begins with established conservation equations, documented fluidized-bed roasting behaviour, and the available thesis simulations. It treats the twin as a proposed framework, selects zinc-sulfide oxidation as the reference metallurgical system, and specifies the models, sensors, validation tests, and evidence required for implementation. The central problem is to connect bed hydrodynamics, reaction chemistry, heat release, measurements, online estimation, and constrained control without presenting unverified benefits as research findings.

II. SCOPE, REVIEW APPROACH, AND EXPLICIT ASSUMPTIONS

➤ *Perspective Method and Evidence Boundary*

This paper is a perspective and engineering framework, not a systematic or critical review. It integrates four evidence domains: industrial fluidized-bed roasting, dense gas–solid modelling, digital-twin architecture and data assimilation, and model-based process control. Peer-reviewed sources and international standards support the technical propositions. Foundational equations remain included when they define current engineering practice. The paper does not claim exhaustive database coverage or a quantitative meta-analysis. Its purpose is to derive an implementable architecture, expose unresolved choices, and define tests capable of rejecting or supporting each central hypothesis.

➤ *Reference Process and Assumptions*

Table 1 Reference Assumptions and Their Evidential Status.

Item	Reference assumption	Status in the proposed framework
Feed	Predominantly ZnS concentrate containing iron sulfides and gangue; mineralogy, elemental composition, moisture, size distribution, density, and sphericity must be measured.	No synthetic composition is assigned.
Reactor	Continuous atmospheric bubbling fluidized bed with distributor, dense bed, freeboard, solids overflow, cyclone, and downstream gas cleaning.	Transient operation is retained.
Temperature	Nominal roasting window 1123–1223 K for framework design; the plant-specific window must follow equilibrium, kinetics, sulfate limits, and agglomeration tests.	Literature-guided range, not a measured result.
Pressure	Near atmospheric pressure with local distributor and bed pressure losses.	Ideal-gas behaviour is acceptable at first pass.
Gas	Air or oxygen-enriched air. Local O_2, SO_2, SO_3, N_2, and water vapour are relevant.	Gas activity is approximated by $p_i/p°$.
Solids	ZnS, ZnO, $ZnSO_4$, FeS_2, FeS, Fe_3O_4, Fe_2O_3, ferrites, and gangue phases.	Solid activities begin at unity for pure phases, then use phase-model corrections when required.
Particles	Polydisperse, reactive, potentially attriting and agglomerating.	Eulerian–Eulerian model online surrogate; CFD–DEM only for offline mechanism studies.
Control objective	Maintain calcine residual sulfide sulfur, temperature, oxygen availability, bed inventory, and emissions within operating constraints.	Objectives and limits require plant approval.

The framework assumes local thermal non-equilibrium in the high-fidelity model because gas and particle temperatures need not coincide during feed heating, reaction, bubble passage, and freeboard transport. It also assumes that steady-state calculations remain useful for initialization and reconciliation, while state estimation and control must remain transient. Activities of gas species use partial pressure divided by standard pressure. Unit solid activity is a first screening approximation, not a substitute for phase-equilibrium modelling of non-ideal ferrites, sulfates, or gangue-containing solids.

III. METALLURGICAL CHEMISTRY AND PHASE EXPECTATIONS

➤ *Principal Reaction Network*

The reference network must represent direct sulfide oxidation, sulfate formation and decomposition, iron-sulfide

ISSN No:-2456-2165 https://doi.org/10.38124/ijisrt/26aug400

oxidation, sulfur trioxide formation, and ferrite formation. The following balanced reactions are a minimum set for model development:

- 2 $ZnS(s) + 3 O_2(g) \rightarrow 2 ZnO(s) + 2 SO_2(g)$
- $ZnS(s) + 2 O_2(g) \rightarrow ZnSO_4(s)$
- 4 $FeS_2(s) + 11 O_2(g) \rightarrow 2 Fe_2O_3(s) + 8 SO_2(g)$
- 3 $FeS_2(s) + 8 O_2(g) \rightarrow Fe_3O_4(s) + 6 SO_2(g)$
- 4 $FeS(s) + 7 O_2(g) \rightarrow 2 Fe_2O_3(s) + 4 SO_2(g)$
- 3 $FeS(s) + 5 O_2(g) \rightarrow Fe_3O_4(s) + 3 SO_2(g)$
- 2 $SO_2(g) + O_2(g) \rightleftharpoons 2 SO_3(g)$
- $ZnO(s) + SO_3(g) \rightleftharpoons ZnSO_4(s)$
- $ZnSO_4(s) \rightleftharpoons ZnO(s) + SO_3(g)$
- $ZnO(s) + Fe_2O_3(s) \rightleftharpoons ZnFe_2O_4(s)$

Direct ZnS oxidation to ZnO is favoured by adequate oxygen supply and temperatures that prevent persistent sulfate accumulation. Sulfate formation becomes more relevant at lower temperature and sufficiently high SO_3 potential. Iron sulfides contribute strongly to heat release and change the oxygen demand. Magnetite becomes more stable at lower oxygen potential than hematite. Zinc ferrite formation can reduce zinc leachability in downstream hydrometallurgical treatment, so the twin must connect temperature and oxygen history to calcine phase quality rather than track conversion alone.

➢ *Dominant States and Measurable Quality Variables*

The minimum metallurgical state vector should include bed temperature distribution, bed inventory, gas and solids holdup, oxygen and sulfur-oxide fields, reaction extents, particle-size distribution, and selected phase fractions. Online instrumentation does not measure most of these states directly. The twin must estimate them from temperature, differential pressure, flow, off-gas analysis, feed measurements, and delayed calcine assays. X-ray diffraction, mineralogical microscopy, elemental sulfur speciation, and leachability tests provide slower validation targets.

➢ *Thermodynamic Feasibility and Operating Window*

Thermodynamics determines feasible phase assemblages and the direction of reactions. It does not determine how rapidly particles reach equilibrium. For reaction j,

$$\Delta G_j = \Delta G_j^\circ + RT\ln Q_j \quad (1)$$

Where ΔG_j is reaction Gibbs energy in J mol⁻¹, ΔG°_j is the standard value in J mol⁻¹, R is 8.314 J mol⁻¹ K⁻¹, T is temperature in K, and Q_j is the dimensionless reaction quotient. At equilibrium,

$$\Delta G_j^\circ = -RT\ln K_j \quad (2)$$

Where K_j is the equilibrium constant. Chemical potential and activity follow

$$\mu_i = \mu_i^\circ + RT\ln a_i, \qquad a_i = \gamma_i x_i, \qquad a_{i,\mathrm{gas}} \simeq \frac{p_i}{p^\circ} \quad (3)$$

Where μ_i is in J mol⁻¹, γ_i is the activity coefficient, x_i is mole fraction, p_i is partial pressure in Pa, and p° is standard pressure. The temperature dependence of equilibrium is summarized by

$$\ln K_j = -\frac{\Delta H_j^\circ}{RT} + \frac{\Delta S_j^\circ}{R} \quad (4)$$

Where ΔH°_j and ΔS°_j are the standard reaction enthalpy and entropy. These relations support oxygen-potential and sulfur-potential diagrams. In qualitative terms, oxidation of ZnS and iron sulfides remains strongly favourable in an oxidizing roaster. The practical selectivity problem is not whether oxidation occurs. It is whether the local combination of temperature, pO_2, pSO_2, and pSO_3 produces ZnO, retained $ZnSO_4$, hematite, magnetite, or zinc ferrite at the particle scale.

A defensible twin should therefore contain an equilibrium screening service. At each reconciled operating point it computes reaction quotients and phase-stability margins. The service should flag proximity to sulfate persistence, reduced iron oxides, or ferrite-forming conditions. Equilibrium calculations should use a validated thermochemical database. The published manuscript should identify the database version, solution models, species set, and suppressed phases. Without these details, equilibrium plots are not reproducible.

The provisional 1123–1223 K range provides a starting window for zinc-sulfide roasting, but it is not universal. Lower temperature increases the risk of slow conversion and sulfate persistence. Higher temperature accelerates reaction and sulfate decomposition but raises the probability of sintering, agglomeration, refractory loading, and volatile-species transfer. Feed mineralogy and downstream leaching requirements determine the final window. The correct set point is therefore a constrained region, not a single temperature.

IV. KINETICS, TRANSPORT, AND FLUIDIZATION

➢ *Particle Reaction and Transport*

Reaction rates depend on chemical kinetics, oxygen transport through the external film, diffusion through porous or product layers, heat transfer, and evolving particle structure. A general Arrhenius rate constant is

$$k_j = A_j \exp\left(-\frac{E_{a,j}}{RT}\right) \quad (5)$$

Where k_j has units consistent with the selected rate law, A_j is the pre-exponential factor, and $E_{a,j}$ is activation energy in J mol⁻¹. A practical heterogeneous rate expression is

$$r_{j,A} = k_j f\left(a_{\mathrm{ZnS}}, p_{\mathrm{O_2}}, p_{\mathrm{SO_2}}, p_{\mathrm{SO_3}}, X, \varepsilon_p\right), \qquad R_j = a_v r_{j,A} \quad (6)$$

ISSN No:-2456-2165 https://doi.org/10.38124/ijisrt/26aug400

Where $r_{j,A}$ is the surface rate in mol m⁻² s⁻¹, a_v is reactive surface area per reactor volume in m² m⁻³, and R_j is the volumetric molar rate in mol m⁻³ s⁻¹. A mass-specific law $r_{j,m}$ in mol kg⁻¹ s⁻¹ is converted through $R_j = \rho b\, r_{j,m}$, where ρb is reactive bulk-solids concentration in kg m⁻³. X is conversion and εp is particle porosity. The energy and species balances must use R_j, not an area-specific or mass-specific rate without conversion. The kinetic function must be fitted over the intended temperature, oxygen potential, particle-size, and conversion ranges.

For external mass transfer,

$$N_i = k_m A_p (C_{i,b} - C_{i,s}), \qquad \mathrm{Sh} = \frac{k_m d_p}{D_i} = f(\mathrm{Re}_p, \mathrm{Sc}) \tag{7}$$

Where N_i is molar transfer rate in mol s⁻¹, k_m is mass-transfer coefficient in m s⁻¹, A_p is particle area in m², C is concentration in mol m⁻³, Sh is Sherwood number, d_p is particle diameter in m, D_i is diffusivity in m² s⁻¹, Re_p is particle Reynolds number, and Sc is Schmidt number. Internal diffusion is screened with an effectiveness factor and Thiele modulus. If a dense product layer forms, a shrinking-core or grain model should be compared against random-pore alternatives. Control by chemical reaction predicts a strong Arrhenius temperature response. Product-layer diffusion produces a weaker apparent temperature dependence and characteristic conversion-time curvature. Gas-film control becomes more relevant for large particles, depleted oxygen, or poor contacting. (Bergman et al., 2017).

➢ *Minimum Fluidization and Pressure Drop*

Before incipient fluidization, the Ergun relation links pressure gradient and superficial velocity:

$$\frac{\Delta P}{L} = 150\frac{\mu_g (1-\varepsilon)^2 U}{\varepsilon^3 \phi_s^2 d_p^2} + 1.75\frac{\rho_g (1-\varepsilon) U^2}{\varepsilon^3 \phi_s d_p} \tag{8}$$

Where ΔP is pressure drop in Pa, L is bed depth in m, µg is gas viscosity in Pa s, ε is voidage, U is superficial gas velocity in m s⁻¹, ρg is gas density in kg m⁻³, and φs is particle sphericity. For a polydisperse concentrate, d_p must be defined through a defensible surface-volume mean or represented by solids classes. At minimum fluidization, (Grace et al., 2020).

$$\Delta P_{mf} = (\rho_s - \rho_g)(1 - \varepsilon_{mf}) g L_{mf} \tag{9}$$

Where ρs is particle density in kg m⁻³ and g is gravitational acceleration in m s⁻². The twin should not infer $U_m f$ from one pressure plateau alone. It should reconcile hot-gas properties, inventory, particle-size distribution, and distributor pressure loss. A practical bubbling-bed operating velocity often lies at a multiple of $U_m f$, but the allowable ratio must be established for the specific concentrate because entrainment, elutriation, bubble growth, and cyclone loading rise with velocity.

➢ *Multiphase Conservation Equations*

For phase q in an Eulerian–Eulerian description, mass conservation is

$$\frac{\partial(\varepsilon_q \rho_q)}{\partial t} + \nabla \cdot (\varepsilon_q \rho_q \mathbf{u}_q) = \dot{m}_q \tag{10}$$

Where εq is volume fraction, ρq is density in kg m⁻³, uq is velocity in m s⁻¹, and ṁq is net mass source in kg m⁻³ s⁻¹. Momentum conservation is.

$$\frac{\partial(\varepsilon_q \rho_q \mathbf{u}_q)}{\partial t} + \nabla \cdot (\varepsilon_q \rho_q \mathbf{u}_q \mathbf{u}_q) = -\varepsilon_q \nabla p + \nabla \cdot \boldsymbol{\tau}_q + \varepsilon_q \rho_q \mathbf{g} + \sum_p \mathbf{M}_{pq} \tag{11}$$

Where p is pressure in Pa, τq is the phase stress tensor in Pa, and Mpq is interphase momentum exchange in N m⁻³. Species transport is

$$\frac{\partial(\varepsilon_g \rho_g Y_i)}{\partial t} + \nabla \cdot (\varepsilon_g \rho_g \mathbf{u}_g Y_i) = \nabla \cdot (\varepsilon_g \rho_g D_{i,\mathrm{eff}} \nabla Y_i) + R_i \tag{12}$$

Where Yi is mass fraction, Di,eff is effective diffusivity in m² s⁻¹, and Ri is reaction source in kg m⁻³ s⁻¹. A two-temperature energy formulation is required when gas and solids are not locally equilibrated:

$$\frac{\partial(\varepsilon_q \rho_q h_q)}{\partial t} + \nabla \cdot (\varepsilon_q \rho_q \mathbf{u}_q h_q) = \nabla \cdot (k_{q,\mathrm{eff}} \nabla T_q) + H_{pq} + S_{q,\mathrm{rxn}} - S_{q,\mathrm{loss}} \tag{13}$$

Where hq is specific enthalpy in J kg⁻¹, kq,eff is effective thermal conductivity in W m⁻¹ K⁻¹, Hpq is interphase heat exchange in W m⁻³, Sq,rxn is reaction heat source, and Sq,loss represents radiation and wall losses. The reactor-scale energy balance provides an independent audit:

$$\frac{dE}{dt} = \sum_{\mathrm{in}} \dot{m}\, h - \sum_{\mathrm{out}} \dot{m}\, h + \sum_j (-\Delta H_{r,j}) R_j V - Q_{\mathrm{wall}} - Q_{\mathrm{rad}} \tag{14}$$

Here R_j is volumetric molar reaction rate. Interphase heat exchange must cancel between phase equations, Hgs + Hsg = 0, so it is absent from the summed reactor balance. Qwall and Qrad are net external conductive-convective and radiative losses in W. Feed sensible heating, moisture evaporation, calcine enthalpy, and off-gas enthalpy enter through the inlet and outlet terms or explicit source terms under one stated convention. Every high-fidelity simulation should close mass, elemental, and energy balances before local contours are interpreted. (Moukalled et al., 2016).

V. MULTIPHYSICS MODEL HIERARCHY

➢ *Offline High-Fidelity Layer*

The proposed primary design model is a transient three-dimensional Eulerian–Eulerian CFD model with kinetic-theory closures for granular stresses, multiple solids classes, reaction sources, interphase heat and mass transfer, wall heat loss, and a resolved or properly characterized distributor.

ISSN No:-2456-2165 https://doi.org/10.38124/ijisrt/26aug400

Dash, Mohanty, and Mishra demonstrated the value of this approach for an industrial continuous zinc roaster and validated model predictions against plant conditions. Their work also shows that industrial geometry and several solids classes matter. Such a model is suitable for design studies and generation of training trajectories, but its computational cost usually prevents direct execution at the plant sampling interval. Closure selection must be tested rather than treated as a software default. Drag, wall specularity, restitution, friction, turbulence modulation, granular conductivity, and interphase heat-transfer correlations all influence predicted circulation and temperature. Mesh independence, time-step independence, statistical averaging, and boundary-condition uncertainty should be reported separately. CFD–DEM belongs in an offline research tier for distributor jets, segregation, agglomeration precursors, and wall interactions. Large-eddy simulation is appropriate only when the research question and computational resolution justify it. Neither method should be described as implemented without solver files and validation evidence. (Celik et al., 2008; Eça and Hoekstra, 2014; Ferziger et al., 2020).

➢ *Online Reduced-Order Layer*

Online execution requires a reduced-order model, compartment model, response-surface surrogate, or physics-informed state-space representation. Reduction should preserve elemental balances, reaction heat, monotonic physical responses, and operating constraints. A purely statistical model trained within a narrow historical window risks extrapolation failure after feed or equipment changes. A hybrid model is preferable. Conservation equations define the backbone, while selected heat-transfer coefficients, reaction multipliers, residence-time parameters, or residual terms are updated from data.

A discrete nonlinear state model is

$$\mathbf{x}_{k+1} = f(\mathbf{x}_k, \mathbf{u}_k, \mathbf{d}_k, \boldsymbol{\theta}_k) + \mathbf{w}_k, \qquad \mathbf{y}_k = h(\mathbf{x}_k, \mathbf{u}_k, \boldsymbol{\theta}_k) + \mathbf{v}_k \tag{15}$$

Where x is the state vector, u denotes manipulated variables, d denotes measured disturbances, θ contains uncertain parameters, y denotes measurements, and w and v are process and measurement errors. Candidate states include zone temperatures, oxygen inventory, reaction extents, solids inventory, particle-class holdup, and fouling or heat-loss factors. The model structure must be observable from the selected sensors before online estimation is attempted.

➢ *Comparative Model Selection*

Table 2. Comparative Role of Candidate Models in the Proposed Hierarchy.

Method	Resolution	Online speed	Data demand	Recommended role
Eulerian–Eulerian CFD	Reactor fields after validation	Low	High	Design, scale-up, and trajectory generation
CFD–DEM	Particle-resolved mechanisms	Very low	High	Offline segregation, collision, and agglomeration studies
Compartment model	Zone-averaged states	High	Moderate	Online balances and state estimation
Pure machine learning	Empirical input-output mapping	High	High and campaign-specific	Bounded interpolation and residual diagnostics
Hybrid reduced-order model	Conservation backbone plus learned correction	High	Moderate	Preferred online prediction and advisory control

➢ *Proposed Digital-Twin Architecture*

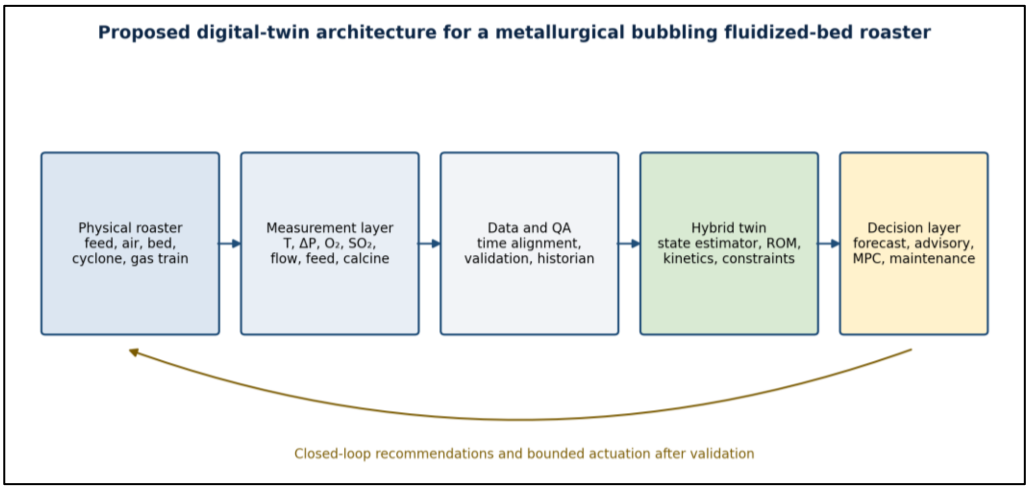

Fig 1 Proposed Architecture and Direction of Information Flow. Closed-Loop Actuation is Permitted Only After Advisory-Mode Validation.

ISSN No:-2456-2165 https://doi.org/10.38124/ijisrt/26aug400

➢ *Physical Asset and Measurement Layer*

The physical boundary should include the concentrate feeder, fluidizing-air system, oxygen enrichment, distributor, dense bed, freeboard, calcine overflow, cyclone return or discharge, waste-heat section, and gas analysis train. Excluding the feed and gas-conditioning delays would break mass-balance and dynamic interpretation. Each tag requires an engineering unit, calibration history, sampling interval, quality code, and time stamp synchronized to a common clock.

Table 3 Minimum Measurement System and Principal Data-Quality Risks.

Variable	Instrument or assay	Role in the twin	Primary failure mode
Bed and freeboard temperature	Shielded thermocouples; selected optical or suction-pyrometer checks	Energy state, gradients, hotspot detection	Drift, radiation bias, coating, location bias
Distributor and bed ΔP	Differential-pressure transmitters and high-frequency pressure channels	Inventory, fluidization regime, blockage and bubble signatures	Impulse-line blockage, zero drift, aliasing
Air and oxygen flow	Mass or compensated volumetric flow measurement	Oxygen balance and manipulated input	Composition compensation, valve stiction
Off-gas O_2, SO_2 and CO_2	Conditioned continuous gas analysers	Conversion, oxygen excess, elemental reconciliation	Transport delay, condensation, calibration drift
Feed rate and moisture	Gravimetric feeder; periodic moisture assay	Mass and energy disturbance	Feeder bias, segregation, delayed assay
Feed and calcine chemistry	XRF, sulfur speciation, XRD, mineralogy, leachability	Delayed quality target and model correction	Sampling error, laboratory delay, phase quantification bias
Particle size and dust rate	Screening or laser sizing; cyclone and dust mass	Hydrodynamic class distribution and attrition	Nonrepresentative sampling

➢ *Data Quality, Reconciliation, and Context*

Raw tags should not enter the estimator without validation. The data service must detect impossible ranges, frozen values, spikes, missing values, time misalignment, analyser transport delay, and maintenance states. Elemental balances provide redundancy. Zinc, iron, sulfur, oxygen, and total mass reconciliation should produce adjusted values and residual diagnostics. Persistent sulfur-balance error may indicate feed-sampling bias, gas-analyser drift, dust losses, or an incomplete reaction network. The twin must retain both raw and reconciled data, including the correction magnitude.

➢ *State and Parameter Estimation*

An extended Kalman filter, unscented Kalman filter, ensemble Kalman filter, or moving-horizon estimator may update unmeasured states and uncertain parameters. Selection depends on nonlinearity, computational budget, constraints, and error distributions. A generic Kalman measurement update is

$$\hat{x}_{k|k} = \hat{x}_{k|k-1} + K_k\left[y_k - h\left(\hat{x}_{k|k-1}\right)\right] \quad (16a)$$

$$P_{k|k} = (I - K_k H_k)P_{k|k-1}(I - K_k H_k)^T + K_k R_k K_k^T \quad (16b)$$

Where $\hat{x}$ is the estimated state, Kk is estimator gain, P is error covariance, H is the local measurement sensitivity matrix, Rk is measurement-noise covariance, and the bracketed term is the innovation. The Joseph covariance form in Equation 16b preserves symmetry and positive semidefiniteness more reliably under finite-precision computation. Structural observability should be assessed before parameter fitting. Empirical observability and parameter identifiability should then be tested under approved input excitation, realistic analyser delay, missing data, and correlated disturbances. Innovation mean, variance, autocorrelation, and cross-correlation provide continuous evidence of model adequacy.

➢ *Twin Services and Control*

The first operational services should be state estimation, soft sensing, fault detection, and short-horizon forecasting. Advisory optimization should follow. Closed-loop model-predictive control should be the final stage after independent safety review. A typical objective is

$$J = \sum_{i=1}^{N_p} (y_{k+i} - r)^T Q (y_{k+i} - r) + \sum_{i=0}^{N_c-1} \Delta u_{k+i}^T R \Delta u_{k+i} + \rho \parallel s \parallel_1 \quad (17)$$

Subject to umin ≤ u ≤ umax, Δumin ≤ Δu ≤ Δumax, Tmin ≤ T ≤ Tmax, and product and emission constraints. Here Np is prediction horizon, Nc is control horizon, r is target, Q and R are weighting matrices, s is a slack variable, and ρ is a penalty. Manipulated variables may include total air, oxygen enrichment, air split, feed rate, and auxiliary fuel during start-up. Hard safety interlocks remain outside the optimizer. The digital twin must never replace independent burner-management, oxygen, pressure, or emergency-shutdown protections.

➢ *Start-up Heating as the First Operating Mode of the Twin*

The accompanying thesis provides a focused basis for the cold start-up module. This mode precedes sulfide concentrate admission and therefore excludes the reaction network of Section 3 from the reported CFD cases. The initial bed is treated as inert particulate material near 298 K. Burner heat input and fluidization airflow govern the transient response, while the distributor, bed inventory, refractory thermal inertia, exhaust sensible heat, and wall losses define the principal constraints. The start-up module should hand

ISSN No:-2456-2165 https://doi.org/10.38124/ijisrt/26aug400

over to the reactive roasting module only after temperature, pressure-drop, burner, draft, and gas-composition permissives have been satisfied. (Rumbu Kayimbu Mutombo, 2025).

For a spatially averaged start-up model, the coupled thermal inventory is represented by

$$C_{\mathrm{th,sys}} \frac{dT_b}{dt} = \dot{Q}_{\mathrm{burner}} + \dot{Q}_{\mathrm{air}} - \dot{Q}_{\mathrm{exhaust}} - \dot{Q}_{\mathrm{wall}} - \dot{Q}_{\mathrm{other}} \quad (18)$$

Where Cth,sys is the effective heat capacity of bed, internals, and participating refractory in J K^{-1}; Tb is representative bed temperature in K; and each heat-rate term is in W. The apparent mean heating rate and a spatial temperature-uniformity index are

$$\bar{\dot{T}} = \frac{T_b(t_2) - T_b(t_1)}{t_2 - t_1}, \qquad \sigma_T = \sqrt{\frac{1}{N}\sum_{i=1}^{N}\left(T_i - \bar{T}\right)^2} \quad (19)$$

The thesis reports that the continuous case Steady_1 reaches approximately 800 K in 1,200 s from an initial value near 298 K. Equation 19 gives an apparent mean heating rate of approximately 0.42 K s^{-1}. During the first 400 s, the tested complete-interruption sequences oscillate between approximately 298 and 308 K. Even the favourable 10 K net rise corresponds to no more than approximately 0.025 K s^{-1}. The ratio of these apparent indicators is near 17. It is a thermal-response comparison, not a fuel-saving factor. The comparison is also limited by unequal simulation durations and the absence of synchronized fuel-flow and pressure-drop measurements. (Rumbu Kayimbu Mutombo, 2025).

The 800 K endpoint is approximately 527 °C. It remains below the thesis terminal start-up interval of 823–873 K, or 550–600 °C. The simulation therefore establishes neither completion of start-up nor readiness for feed admission. It identifies a defensible baseline strategy and the measurements required for the next validation stage.

Table 4 Thesis-Derived Hierarchy of Start-up Airflow Strategies and Evidence Status.

Strategy	Evidence class	Interpretation	Role in the digital twin
C0, continuous constant	Available CFD reference	Stable thermal and hydrodynamic baseline	Retain as fallback and validation reference
P0, complete interruption	Available simulated contrast	Reduced blower-on time but insufficient net heating; defluidization risk	Reject as autonomous industrial mode
R1, reduced continuous ramp	Proposed test	Limits excess cold-air heat loss while preserving a nonzero base flow	First instrumented strategy to test
P1, bounded pulsation	Concept only	Modulates mixing around a nonzero base flow	Test only after R1 and pressure-drop validation
H1, constrained hybrid	Concept only	Coordinates burner, airflow, temperature, and pressure constraints	Longer-term twin-control target

The start-up case supports one bounded proposition for experimental testing: relative to complete airflow interruption, a strategy maintaining a nonzero fluidization baseline should improve net bed heating while preserving pressure-drop stability. This proposition does not establish lower total energy consumption. It must be tested through equal-duration C0, R1, and P1 cases with identical initial bed inventory, burner boundary conditions, wall-loss models, and synchronized fuel, electrical, temperature, and pressure measurements.

The start-up state vector should contain bed and refractory temperatures, temperature dispersion, bed pressure drop, distributor pressure drop, bed inventory, burner duty, total air, draft, and estimated heat-loss coefficients. Burner duty and airflow are manipulated variables. Initial bed mass, moisture, ambient temperature, refractory condition, and gas-analysis delay act as disturbances or uncertain parameters. Minimum fluidization, burner-management logic, maximum refractory heating rate, negative draft, and high-temperature limits remain hard constraints. This mode-specific formulation converts the thesis from background material into a testable first module of the proposed digital twin.

➢ *Verification, Validation, and Uncertainty Framework*

Verification asks whether equations are solved correctly. Validation asks whether the selected equations and parameters represent the roaster for the intended decision. Calibration estimates parameters. These activities must remain distinct. A model calibrated and evaluated on the same operating period has not demonstrated predictive performance. (Oberkampf and Roy, 2010).

Table 5 Staged Verification and Validation Programme.

Stage	Required work	Acceptance evidence
1. Start-up baseline	Repeat C0 over equal durations and initial conditions with totalized fuel, blower electricity, multi-level temperatures, ΔP, draft, initial bed state, and synchronized clocks. Complete at least three instrumented reference campaigns.	Closed thermal balance with stated uncertainty; repeatable temperature and pressure histories; documented run-to-run variability.

ISSN No:-2456-2165 https://doi.org/10.38124/ijisrt/26aug400

2. Data and balances	Instrument calibration, gas delay, mass and elemental closure	Traceable calibration records; bounded reconciliation residuals
3. Hydrodynamics	Cold and hot pressure drop, bed expansion, pressure spectra, solids inventory	Independent validation across gas velocities and inventories
4. Thermal model	Heat-loss tests, axial and radial temperatures, start-up and feed disturbances	Energy closure and credible uncertainty bands
5. Reaction model	TGA or microreactor kinetics, mineralogy, sulfur conversion, sulfate and ferrite formation	Parameter confidence intervals and out-of-sample prediction
6. Integrated CFD	Coupled ΔP, temperature, off-gas, residence time, and calcine quality	Mesh and time-step independence; withheld-condition validation
7. Start-up alternatives	Compare equal-duration C0 and R1 cases first. Test P1 or H1 only after minimum-fluidization and pressure-drop criteria are validated. Keep initial bed mass, thermal state, burner duty, wall conditions, and simulation controls equivalent.	No loss of fluidization; bounded thermal gradients; quantified fuel and blower energy; energy balance closure; tested and documented return to C0.
8. Online estimator	Replay historical transients, missing data, drift, feed changes	Unbiased innovations; stable estimates; fault detection performance
9. Advisory twin	Prospective shadow operation without actuation	Forecast coverage, false alarm rate, operator acceptance
10. Closed-loop trial	Bounded plant trial with rollback and independent interlocks	Constraint compliance and predeclared performance test

Recommended error measures include bias, root-mean-square error, mean absolute error, prediction-interval coverage, and dynamic timing error. R^2 alone is inadequate because it does not reveal bias, conservation error, or transient phase lag. Uncertainty should include measurement error, feed sampling, thermochemical data, kinetic parameters, heat-loss coefficients, boundary conditions, and structural model discrepancy. A practical validation result reports distributions and confidence intervals rather than one aggregate percentage.

Global sensitivity analysis should identify which uncertain inputs dominate calcine sulfur, peak temperature, oxygen slip, and dust loading. Parameters with weak influence should not be estimated online. Parameters with strong influence but poor observability require better measurements or planned excitation tests. The test design should remain within approved operating limits.

➢ *Experimental and Plant Research Programme*

- *Feed and Product Characterization*

Each campaign should quantify elemental composition, sulfur forms, quantitative mineralogy, particle-size distribution, true and bulk density, moisture, porosity, and particle morphology. Calcine characterization should add residual sulfide sulfur, sulfate sulfur, oxide phases, zinc ferrite, particle-size change, dust fraction, and downstream leach response. Composite samples should be linked to exact operating windows and residence-time delays.

- *Bench-Scale Reaction Tests*

Thermogravimetric or differential thermal analysis under controlled O_2–SO_2–N_2 mixtures should separate mass gain by sulfate formation from mass loss by sulfur evolution and sulfate decomposition. Isothermal and non-isothermal tests should cover the proposed operating window and several particle fractions. Replicates, blank corrections, gas calibration, sample mass, heating rate, and external-transfer checks must be reported. Kinetic parameters should be estimated with confidence intervals and tested against withheld conditions.

- *Hydrodynamic and Heat-Transfer Tests (Bergman et al., 2017; Grace et al., 2020).*

A cold model supports distributor mapping, pressure-drop curves, minimum fluidization, mixing, segregation, and entrainment studies. Dynamic similarity should be justified with Archimedes, Reynolds, Froude, and density-ratio arguments rather than geometry alone. A hot pilot provides wall-loss, interphase heat-transfer, reaction, and agglomeration evidence. Pressure fluctuations should be sampled fast enough to retain bubbling signatures. Thermocouples should span axial and radial positions, with documented response time and radiation shielding.

- *Industrial Identification Tests*

Plant tests should use small, approved perturbations in air, oxygen enrichment, feed rate, or air split. Pseudo-random or stepped inputs improve parameter identification when production and safety constraints permit. Each test requires a predeclared protocol, stable feed characterization, time synchronization, analyser-delay estimation, and rollback criteria. Routine historical data alone often contain correlated inputs that prevent unique parameter identification.

VI. PROCESS IMPLICATIONS AND DESIGN RECOMMENDATIONS

➢ *Operating Window*

- Temperature: begin model development over 1123–1223 K, then narrow the window using plant-specific sulfate decomposition, ferrite formation, agglomeration, and conversion evidence.

ISSN No:-2456-2165 https://doi.org/10.38124/ijisrt/26aug400

- Pressure: near atmospheric operation, while retaining measured distributor, dense-bed, freeboard, cyclone, and gas-train pressure losses.
- Gas velocity: establish U/U_{mf} from hot particle properties and entrainment constraints. Do not transfer a fixed multiple from another feed.
- Oxygen potential: maintain sufficient local O_2 for complete oxidation without excessive oxygen enrichment, thermal peaks, or downstream gas-handling burden.
- Particle size: control excessive fines that increase entrainment and broad coarse fractions that increase segregation or incomplete conversion.
- Residence time: estimate a distribution, not a single mean, and relate the low-residence tail to residual sulfide sulfur.

➢ *Principal Risks*

Agglomeration and sintering remain the principal hydrodynamic risks at excessive local temperature or in the presence of low-melting phases. Sulfate persistence compromises calcine quality when temperature and sulfur-oxide potentials favour stable sulfates. Zinc ferrite formation reduces downstream zinc recovery. High gas velocity increases entrainment and gas-cleaning load. Distributor maldistribution produces oxygen-depleted zones and local heat-release differences. Thermocouple drift, plugged pressure lines, and delayed gas analysers can mislead the estimator. The architecture must therefore use redundant signals and explicit sensor-health states.

➢ *Scale-Up*

Scale-up should preserve the mechanisms that govern the target outputs. Geometric similarity alone does not preserve bubble size, solids circulation, wall heat-loss ratio, distributor pressure ratio, or residence-time distribution. The recommended strategy combines dimensionless screening, cold-flow experiments, pilot reaction tests, and validated industrial CFD. Plant calibration should adjust a restricted parameter set. Replacing every uncertain physical term with a fitted coefficient would destroy transferability.

➢ *Digital Governance, Safety, and Lifecycle Management*

A digital twin is a maintained engineering system. Model versions, data lineage, calibration records, software dependencies, access rights, and change approvals must be controlled. Each online recommendation should record the input data, model version, estimator state, constraint set, confidence measure, and operator action. Cybersecurity should segment control networks, authenticate services, minimize write privileges, and retain fail-safe local operation. The twin should degrade safely to monitoring or advisory mode when data quality, uncertainty, or communication latency exceeds limits.

Model-drift monitoring should compare innovations, balance residuals, prediction coverage, and quality-assay errors over time. Trigger conditions should force review after major feed changes, distributor maintenance, refractory repair, analyser replacement, or a sustained change in pressure signatures. The scientific paper should specify these triggers before presenting long-term performance claims.

Economic and environmental assessments should follow implementation, not precede evidence. Economic analysis requires production rate, energy and oxygen prices, maintenance effects, capital cost, discount rate, service life, and a defined baseline. Life-cycle analysis requires functional unit, system boundary, inventory, allocation method, electricity mix, and impact method. Until these data exist, the paper should list evaluation requirements without claiming savings.

➢ *Research Gaps and Testable Hypotheses*

Table 6 Research Gaps Converted into Testable Hypotheses.

Gap	Testable hypothesis	Required test
Observability of internal states	A limited set of temperature, pressure, flow, and gas-composition measurements is sufficient to estimate zone oxygen availability, reaction extent, and inventory with bounded uncertainty.	Test through structural and empirical observability analysis, then validate against withheld calcine and gas data.
Hybrid-model transferability	A conservation-based reduced model with a small learned residual transfers across feed campaigns better than an unconstrained black-box model.	Train on one campaign and test prospectively on mineralogically distinct campaigns.
Pressure signatures	High-frequency differential-pressure features identify distributor maldistribution or agglomeration earlier than conventional mean pressure drop.	Create labelled pilot or maintenance events and compare detection lead time and false alarms.
Phase-quality soft sensor	Combining thermodynamic stability margins with delayed assays improves prediction of sulfate and zinc-ferrite formation.	Compare against purely empirical models using quantitative mineralogy and leachability.
Safe predictive control	A constrained MPC using uncertainty-aware forecasts reduces constraint excursions without increasing dust load or oxygen use.	Evaluate first in simulation, then shadow mode, then bounded prospective trials.
Start-up airflow coordination	Reduced continuous airflow above the validated minimum-fluidization limit yields a better thermal-	Run equal-duration C0, R1, and bounded P1 simulations, then at least three instrumented plant campaigns per accepted strategy.

ISSN No:-2456-2165 https://doi.org/10.38124/ijisrt/26aug400

	hydrodynamic compromise than complete interruption under equivalent start-up conditions.	Compare heating rate, temperature dispersion, ΔP stability, specific start-up energy, and transition permissives.

VII. CONCLUSIONS

A metallurgical fluid-bed roaster qualifies as a strong digital-twin application because hydrodynamics, thermochemistry, reaction kinetics, solids quality, and equipment condition interact across different time scales. It also exposes why a digital twin cannot be reduced to CFD, IoT sensors, or machine learning alone.

- The proposed framework defines five connected layers: physical asset, measurement and data quality, multiphysics and reduced-order models, state and parameter estimation, and decision services.
- Zinc-sulfide roasting provides a coherent reference network that includes oxide, sulfate, iron-oxide, sulfur-trioxide, and ferrite pathways. Phase quality must be estimated alongside conversion.
- Eulerian–Eulerian CFD is the recommended industrial high-fidelity backbone. CFD–DEM and large-eddy simulation remain offline research tools unless their implementation and validation are demonstrated.
- The online model should preserve mass, elemental, and energy balances while estimating a restricted set of uncertain parameters from synchronized plant data.
- Verification, calibration, validation, uncertainty quantification, and prospective shadow operation must precede closed-loop control.
- No energy, economic, environmental, or control improvement is claimed in this framework. Such claims require a defined baseline, traceable data, withheld-condition prediction, and predeclared statistical tests.
- The thesis establishes the cold start-up mode as the first evidence-bearing case within the proposed twin. Its CFD results support C0 as the reference, R1 as the next strategy to test, and P1 or H1 only after hydrodynamic validation. They do not establish fuel savings or complete start-up.

The immediate research priority is to repeat the start-up cases over equal durations and initial conditions. Subsequent work should characterize the feed and calcine, determine reaction and phase behaviour, validate hot-bed hydrodynamics and thermal balances, identify dynamic models from approved plant tests, and demonstrate predictive credibility in advisory mode. This sequence defines a testable research programme.

Author Contributions

Roger Rumbu: Conceptualization, methodology, thesis-derived data interpretation, metallurgical analysis, writing, and supervision. Reggie-John Rumbu: Engineering analysis, model architecture, visualization, and manuscript review.

Funding

This research received no external funding.

Conflicts of Interest

The authors declare no conflict of interest.

Data and Code Availability

No new experimental dataset or simulation code was generated for this framework paper. Future implementation papers should deposit de-identified input data, model configurations, parameter files, and analysis scripts in a persistent repository when industrial confidentiality permits. Any restricted dataset should be described sufficiently for reviewers to assess provenance, calibration, and validation.

REFERENCES

[1]. Bergman, T.L., A.S. Lavine, F.P. Incropera, and D.P. DeWitt. Fundamentals of Heat and Mass Transfer. 8th ed., Wiley, 2017.
[2]. Celik, I.B., U. Ghia, P.J. Roache, C.J. Freitas, H. Coleman, and P.E. Raad. “Procedure for Estimation and Reporting of Uncertainty Due to Discretization in CFD Applications.” Journal of Fluids Engineering, 130, 2008, 078001.
[3]. Chen, Y., O. Yang, C. Sampat, P. Bhalode, R. Ramachandran, and M. Ierapetritou. “Digital Twins in Pharmaceutical and Biopharmaceutical Manufacturing: A Literature Review.” Processes, 8, 2020, 1088.
[4]. Crowe, C.T., J.D. Schwarzkopf, M. Sommerfeld, and Y. Tsuji. Multiphase Flows with Droplets and Particles. 2nd ed., CRC Press, 2012.
[5]. Dash, S., S. Mohanty, and B.K. Mishra. “CFD Modelling and Simulation of an Industrial Scale Continuous Fluidized Bed Roaster.” Advanced Powder Technology, 31, 2020, 658–669.
[6]. Eça, L., and M. Hoekstra. “A Procedure for the Estimation of the Numerical Uncertainty of CFD Calculations Based on Grid Refinement Studies.” Journal of Computational Physics, 262, 2014, 104–130.
[7]. Ferziger, J.H., M. Perić, and R.L. Street. Computational Methods for Fluid Dynamics. 4th ed., Springer, 2020.
[8]. Fuller, A., Z. Fan, C. Day, and C. Barlow. “Digital Twin: Enabling Technologies, Challenges and Open Research.” IEEE Access, 8, 2020, 108952–108971.
[9]. Gaskell, D.R., and D.E. Laughlin. Introduction to the Thermodynamics of Materials. 6th ed., CRC Press, 2018.
[10]. Grace, J.R., X. Bi, and N. Ellis, eds. Essentials of Fluidization Technology. Wiley-VCH, 2020.
[11]. International Organization for Standardization. ISO 23247-1:2021, Automation Systems and Integration: Digital Twin Framework for Manufacturing, Part 1: Overview and General Principles. ISO, 2021.
[12]. International Organization for Standardization. ISO 23247-2:2021, Automation Systems and Integration: Digital Twin Framework for Manufacturing, Part 2: Reference Architecture. ISO, 2021.

ISSN No:-2456-2165 https://doi.org/10.38124/ijisrt/26aug400

[13]. International Organization for Standardization. ISO 23247-4:2021, Automation Systems and Integration: Digital Twin Framework for Manufacturing, Part 4: Information Exchange. ISO, 2021.
[14]. Jarosz, P., and S. Małecki. "Kinetics of the Fluidised Oxidation of Zinc Sulphide Concentrates with an Addition of Inert Materials." Archives of Metallurgy and Materials, 59(4), 2014, 1367–1372. https://doi.org/10.2478/amm-2014-0233.
[15]. Jones, D., C. Snider, A. Nassehi, J. Yon, and B. Hicks. "Characterising the Digital Twin: A Systematic Literature Review." CIRP Journal of Manufacturing Science and Technology, 29, 2020, 36–52.
[16]. Kritzinger, W., M. Karner, G. Traar, J. Henjes, and W. Sihn. "Digital Twin in Manufacturing: A Categorical Literature Review and Classification." IFAC-PapersOnLine, 51(11), 2018, 1016–1022.
[17]. Moukalled, F., L. Mangani, and M. Darwish. The Finite Volume Method in Computational Fluid Dynamics. Springer, 2016.
[18]. Negri, E., L. Fumagalli, and M. Macchi. "A Review of the Roles of Digital Twin in CPS-Based Production Systems." Procedia Manufacturing, 11, 2017, 939–948.
[19]. Oberkampf, W.L., and C.J. Roy. Verification and Validation in Scientific Computing. Cambridge University Press, 2010.
[20]. Rasheed, A., O. San, and T. Kvamsdal. "Digital Twin: Values, Challenges and Enablers from a Modeling Perspective." IEEE Access, 8, 2020, 21980–22012.
[21]. Rhodes, M. Introduction to Particle Technology. 2nd ed., Wiley, 2008.
[22]. Rumbu Kayimbu Mutombo, R. Optimisation du chauffage au démarrage d'un four de grillage à lit fluidisé bouillonnant: Approche intégrée par bilan énergétique, CFD multiphasique et optimisation du soufflage. Master Thesis, Institut Supérieur de Techniques Appliquées, I.S.T.A./Ndolo, 2025.
[23]. Segovia, M., and J. García-Alfaro. "Design, Modeling and Implementation of Digital Twins." Sensors, 22, 2022, 5396.
[24]. Van der Hoef, M.A., M. van Sint Annaland, N.G. Deen, and J.A.M. Kuipers. "Numerical Simulation of Dense Gas–Solid Fluidized Beds: A Multiscale Modeling Strategy." Annual Review of Fluid Mechanics, 40, 2008, 47–70.
[25]. Wang, J., M.A. van der Hoef, and J.A.M. Kuipers. "Why the Two-Fluid Model Fails to Predict the Bed Expansion Characteristics of Geldart A Particles in Gas-Fluidized Beds: A Tentative Answer." Chemical Engineering Science, 64, 2009, 622–625.
[26]. Zhu, H.P., Z.Y. Zhou, R.Y. Yang, and A.B. Yu. "Discrete Particle Simulation of Particulate Systems: Theoretical Developments." Chemical Engineering Science, 62, 2007, 3378–3396.